EMBRY-RIDDLE
Aeronautical University
SCHOLARLY COMMONS

Publications

2013

Heteroclinic and Homoclinic Connections Between the Sun-Earth Triangular Points and Quasi-Satellite Orbits for Solar Observations

Pedro J. Llanos
G.M.V. Aerospace & Defence S.A.U., llanosp@erau.edu

Gerald R. Hintz
University of Southern California

Martin W. Lo
California Institute of Technology

James K. Miller

Follow this and additional works at: https://commons.erau.edu/publication

 Part of the Astrophysics and Astronomy Commons, and the Space Vehicles Commons

Scholarly Commons Citation

Llanos, P. J., Hintz, G. R., Lo, M. W., & Miller, J. K. (2013). Heteroclinic and Homoclinic Connections Between the Sun-Earth Triangular Points and Quasi-Satellite Orbits for Solar Observations. *Journal of Earth Science and Engineering, 3*(8). Retrieved from https://commons.erau.edu/publication/882

This Article is brought to you for free and open access by Scholarly Commons. It has been accepted for inclusion in Publications by an authorized administrator of Scholarly Commons. For more information, please contact commons@erau.edu.

Journal of Earth Science and Engineering 3 (2013) 515-526

Heteroclinic and Homoclinic Connections between the Sun-Earth Triangular Points and Quasi-Satellite Orbits for Solar Observations

Pedro J. Llanos[1,2], Gerald R. Hintz[2], Martin W. Lo[3] and James K. Miller[4]

1. Flight Mechanics Section, GMV Space and Defence, S. A., Tres Cantos, Madrid 28760, Spain

2. Astronautical Engineering Department, University of Southern California, Los Angeles 90089, USA

3. Jet Propulsion Laboratory, California Institute of Technology, Pasadena 91109, USA

4. Retired Chief Scientist, Space Navigation and Flight Dynamics Section, KinetX Inc., Simi Valley, California, 93065, USA

Received: June 15, 2013/Accepted: July 20, 2013/Published: August 25, 2013.

Abstract: Investigation of new orbit geometries exhibits a very attractive behavior for a spacecraft to monitor space weather coming from the Sun. Several orbit transfer mechanisms are analyzed as potential alternatives to monitor solar activity such as a sub-solar orbit or quasi-satellite orbit and short and long heteroclinic and homoclinic connections between the triangular points L4 and L5 and the collinear point L3 of the CRTBP (circular restricted three-body problem) in the Sun-Earth system. These trajectories could serve as channels through where material can be transported from L5 to L3 by performing small maneuvers at the departure of the Trojan orbit. The size of these maneuvers at L5 is between 299 m/s and 730 m/s depending on the transfer time of the trajectory and does not need any deterministic maneuvers at L3. Our results suggest that material may also be transported from the Trojan orbits to quasi-satellite orbits or even displaced quasi-satellite orbits.

Key words: Quasi-satellite orbits, heteroclinic, homoclinic, Sun-Earth triangular points, invariant manifolds, solar observations.

1. Introduction

Heteroclinic and homoclinic connections are of special interest for space mission applications, such as low energy orbits to the Moon [1] and the Petit Grand Tour to the moons of Jupiter [2]. We know that in the Earth-Moon system [3] a spacecraft in orbit near the triangular points L4 and L5 can migrate back and forth between these points through the collinear point L3 without encountering the Moon. Similarly, a spacecraft in the Sun-Earth system can exhibit this motion, which has recently been observed in asteroids. The first Earth Trojan asteroid [4] (2010 TK7) was discovered in 2010 by the WISE (wide infrared survey spacecraft) spacecraft. This ECA (Earth co-orbital asteroid) is in a 1:1 mean motion resonance with the Earth, that is, it goes around the Sun in the same amount of time as the Earth. Asteroid 2010 TK7 has an approximately 390-year cycle. Currently, this asteroid orbits in tadpole-shaped loops around L4. These loops are large, reaching as close as 2,000,000 km from Earth (about 50 times the distance from the Earth to the Moon) and nearly as far as the opposite side of the Sun from the Earth. Eventually, the motion of 2010 TK7 will reverse direction and come back to its current position. Irregular motion of this type of orbit will be analyzed in some examples in this paper. But there are many more asteroids following a horseshoe orbit motion, such as asteroids 2003 YN107 and 2010 SO16. These asteroids are in 1:1 resonance with the Earth because they share Earth's orbit. So,

Corresponding author: Pedro J. Llanos, Marie Curie senior researcher fellow, main research fields: astrodynamics, orbital mechanics, applications to space mission design, comets, asteroids, astrophysics. E-mail: pedro.j.llanos.1@gmail.com.

when they are in front of the Earth, they are slowed down and they are accelerated when they are behind the Earth.

2. Motivation

In previous papers [5, 6], we investigated possible transfer trajectories and orbits around the triangular points (Trojan orbits) that are coplanar with the ecliptic plane. We also analyzed [7] other orbits (above or below the ecliptic) that are displaced from L5, called "sub-L5 orbits" (Fig. 1h) that are more attractive from a science perspective because a spacecraft in any of these orbits could anticipate space weather up to 7 days earlier than its arrival at Earth.

Other nominal Trojan orbits provide only a 3-5 day advance warning at the Earth. Some of these orbits are the planar Trojan orbits illustrated in Fig. 1a and the three-dimensional Trojan orbit displayed in Fig. 1g.

Other planar elliptical Trojan orbits were found around L5 as shown in Fig. 1b. These orbits can be as large as 370,000 km and as small as 30,000 km in amplitude. Finally, asymmetric orbits [7] were differentially corrected with amplitudes of about 120,000 km and 150,000 km (Figs. 1e and 1f), respectively.

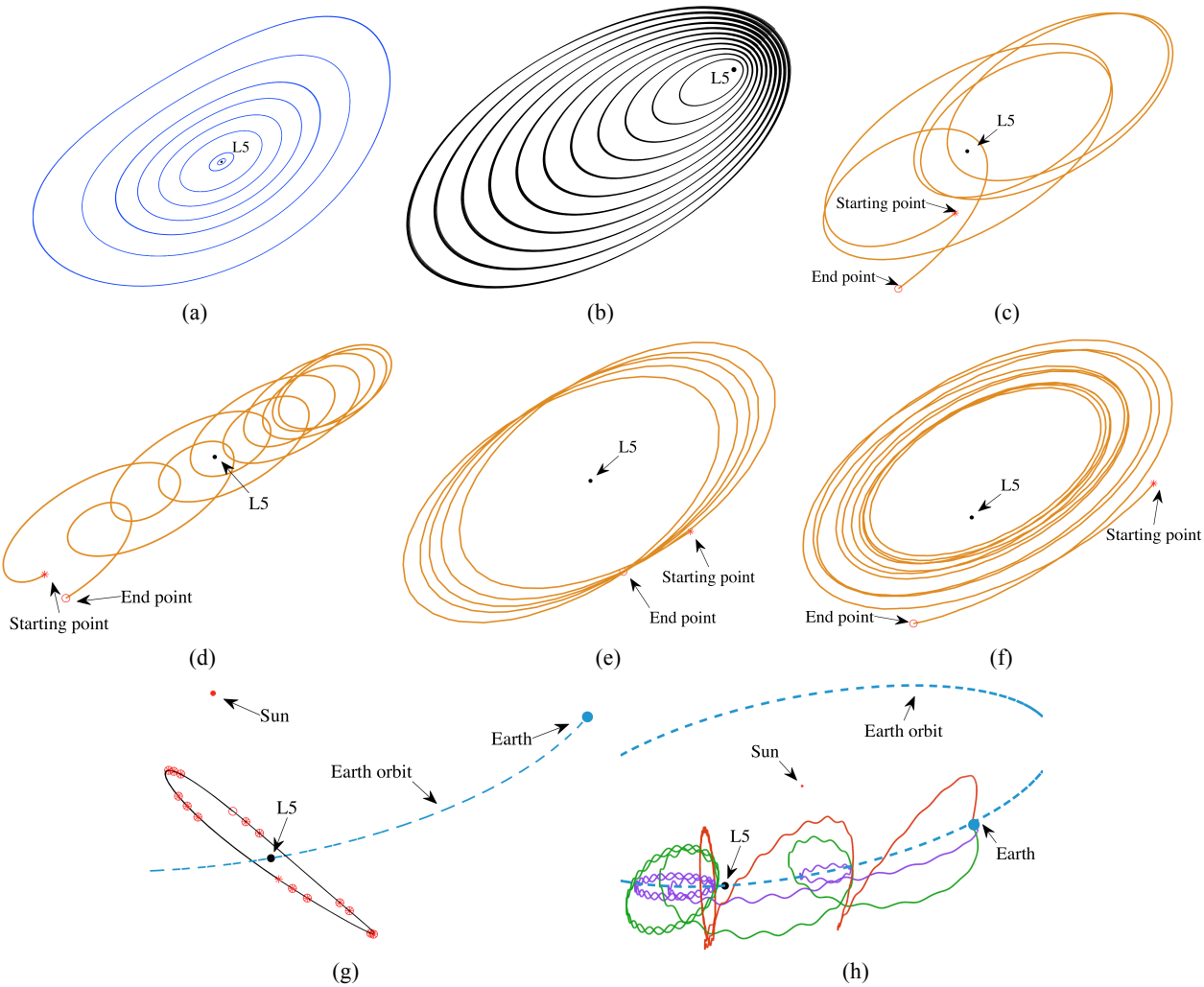

Fig. 1 Different orbit geometries for solar observations: (a) peanut-shape Trojan orbits around L5; (b) elliptical Trojan orbits with L5 being a focus of each ellipse; (c) short-lived tadpole orbit around L5; (d) long-lived tadpole orbit around L5; (e) asymmetric Trojan orbit around L5; (f) Trojan orbit around L5 spiraling in and out of L5 vicinity; (g) three-dimensional differentially corrected Trojan orbit around L5; (h) integrated sub-L5 Trojan orbits.

Although some of these orbits are very promising in studying solar events, there are other orbits where the spacecraft does not need to be strictly off the ecliptic plane, requiring less ΔV and therefore yielding a lower mission cost. This paper will address some of these orbits in the ecliptic plane as shown in Fig. 2a, potential powered heteroclinic connections between the triangular points, and powered heteroclinic connections between the triangular points and the collinear point L3 in the Sun-Earth system.

Besides the tadpole Trojan (Figs. 1c and 1d) and horseshoe motion [7], we could place a satellite into a retrograde QS (quasi-satellite) motion as shown by some of the orbits displayed in Fig. 2a.

A quasi-satellite is an object near an unstable 1:1 resonance of the planet and remains close to the planet during the quasi-satellite phase. The QS orbit (green) is a simulated differentially corrected [8] trajectory depicted in Fig. 2a with an amplitude of $A_y = 2\ A_x = 0.85$ AU as seen in the rotating frame from the Earth. In Fig. 2b, we exhibit a schematic of a quasi-satellite orbit recommended by the scientists [9] as an attractive option for both an operational space weather perspective and a research perspective. Similar to the sub-L5 orbits [7], which can anticipate space weather up to a week in advance of the Earth, which is sooner than reception in a Trojan orbit around L5, these quasi-satellite orbits (sub-L1 orbits) can also anticipate space weather earlier than other orbits around L_1.

Some of these orbits are placed closer to the Sun than other orbits located around the collinear point L1. These closer orbits will provide advance warning of solar events and CMEs (Coronal Mass Ejections) coming toward the Earth. In the rotating coordinate system, a spacecraft located in a quasi-satellite orbit appears to orbit (oval shape) the Earth (Fig. 2a), but it is actually orbiting in a heliocentric orbit around the Sun as seen in inertial coordinates. This quasi-satellite orbit (sometimes called a retrograde orbit) is relatively close to the Earth-Sun line. A constellation of satellites

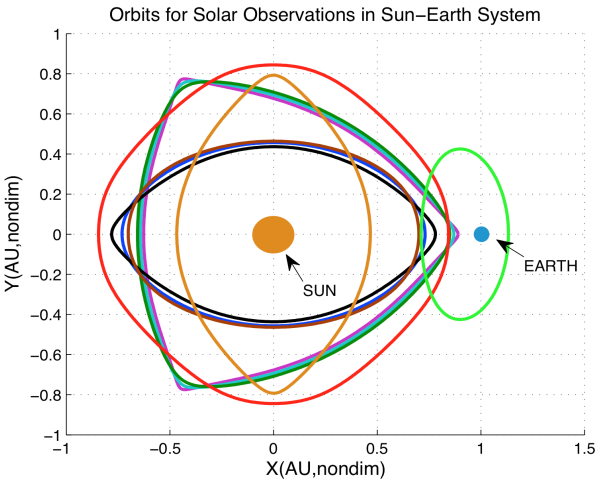

(a)

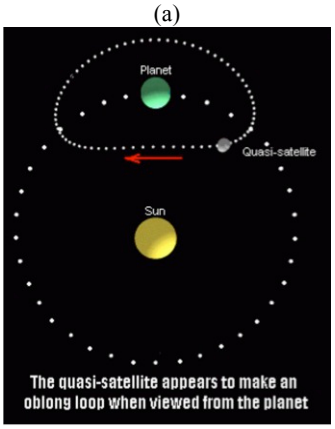

(b)

Fig. 2 (a) Several shapes of simulated quasi-satellite orbits as seen in the corotating frame. The green orbit is a simulated quasi-satellite orbit; (b) artist's conception of a QSO (quasi-satellite orbit) around the Earth.

can be arranged so that at least one spacecraft will be closer to the Sun than the Earth while providing continuous transmission of solar conditions. This orbit geometry will help to anticipate space weather, which generates geomagnetic storms and other interplanetary disturbances that can disrupt communications in our infrastructures on Earth and endanger future human space flights.

3. Model and Methodology

We used the CRTBP (circular restricted three-body problem) in the trajectory analysis for this study [10]. The Sun is the primary body, the Earth is the secondary body and the spacecraft is the third body or infinitesimal mass in this system. To simplify the

analysis, we used the normalized and non-dimensionalized convention so that the mass of the secondary body is $0 < \mu < 1$ and the mass of the primary body is $1 - \mu$. The distance between the primary and secondary bodies is normalized to 1 with the primary body located on the x-axis at $-\mu$ and the secondary body at $1 - \mu$. The x-axis is directed from the primary body to the secondary body. The y-axis is 90° from the x-axis in the primary plane of motion. Finally, the z-axis completes the right-handed system, defining the out-of-plane direction. For this work, μ = 3.040423389123456E-6 for the Earth-Moon barycenter model based on the combined mass of the Earth and Moon, $M_{EMbaryc}$, using JPL DE405 constants. Finally, time corresponds to the angle between the x-axis of the rotating frame and the x-axis of the inertial frame so that the period of the rotating frame becomes 2π. Using this convention, the motion of the infinitesimal mass in the rotating frame can be described by the governing equations of motion:

$$\begin{aligned} \ddot{x} - 2\dot{y} &= x - (1-\mu)\frac{x+\mu}{r_1^3} - \mu\frac{x-1+\mu}{r_2^3} \\ \ddot{y} + 2\dot{x} &= \left(1 - \frac{(1-\mu)}{r_1^3} - \frac{\mu}{r_2^3}\right) y \\ \ddot{z} &= -\left(\frac{(1-\mu)}{r_1^3} - \frac{\mu}{r_2^3}\right) z \end{aligned} \tag{1}$$

where r_1 is the distance from the spacecraft to the Sun and r_2 is the distance from the spacecraft to the Earth,

$$\begin{aligned} r_1 &= \sqrt{(x+\mu)^2 + y^2 + z^2} \\ r_2 &= \sqrt{(x-1+\mu)^2 + y^2 + z^2} \end{aligned} \tag{2}$$

and

$$\mu = \frac{M_{EMbaryc}}{M_{EMbaryc} + M_s} \tag{3}$$

where M_s denotes the mass of the Sun. The CRTBP is nondimensionalized so that the sum of the primary and secondary masses, the mean motion of the rotating frame, the distance between the primary and secondary, and the gravitational constant are all unity. In the last section of this work, we will analyze other orbit geometries using low thrust. For this, we use similar two-body equations of motion in polar coordinates [11] described below:

$$\begin{aligned} \ddot{r} &= r\dot{\theta}^2 - \frac{\mu_{Earth}}{r^2} \\ \ddot{\theta} &= \frac{1}{r}\left(-2\dot{r}\dot{\theta} + \frac{T}{m}\right) \end{aligned} \tag{4}$$

where r is the spacecraft's distance from the central body (in this case Earth), θ is the true anomaly (angular distance) of the spacecraft's position in the orbit, μ_{Earth} is the mass parameter of the Earth, m is the varying mass of the spacecraft due to the T (thrust), which is assumed to be in the tangential direction, g_0 is the gravity at Earth and I_{sp} is the specific impulse. The mass variation is governed by:

$$\dot{m} = -\frac{T}{g_0 I_{sp}} \tag{5}$$

4. Results

In this section, we provide the results for the powered heteroclinic and homoclinic connections between the triangular points and the collinear point L3 in the Sun-Earth system. Then, we will show the results for the quasi-satellite orbits as potential orbits for solar observations. Finally, some other orbit geometries are delivered. Fig. 3 illustrates the manifolds from the triangular points in the Sun-Earth system for a given Trojan orbit of amplitude 0.52 AU. When generating manifolds that depart from or arrive to the halo orbits around the unstable collinear points, an offset of 200 km from the orbit works very well to generate these manifolds. However, this offset does not yield any realistic manifolds around the stable triangular points due in part with the stability properties [10] associated with the Trojan orbits around L5. Therefore, we used different offsets yielding the manifolds depicted in Fig. 3. Because L4 and L5 orbits are weakly unstable, their invariant manifolds take thousands years to reach from L4 to L5. Our investigation of some of these manifolds suggests that we cannot use these invariant manifolds or ultra-low-energy trajectories for a space mission. Our analysis suggests that unlike halo orbits, the invariant manifolds of Earth Trojan orbits are

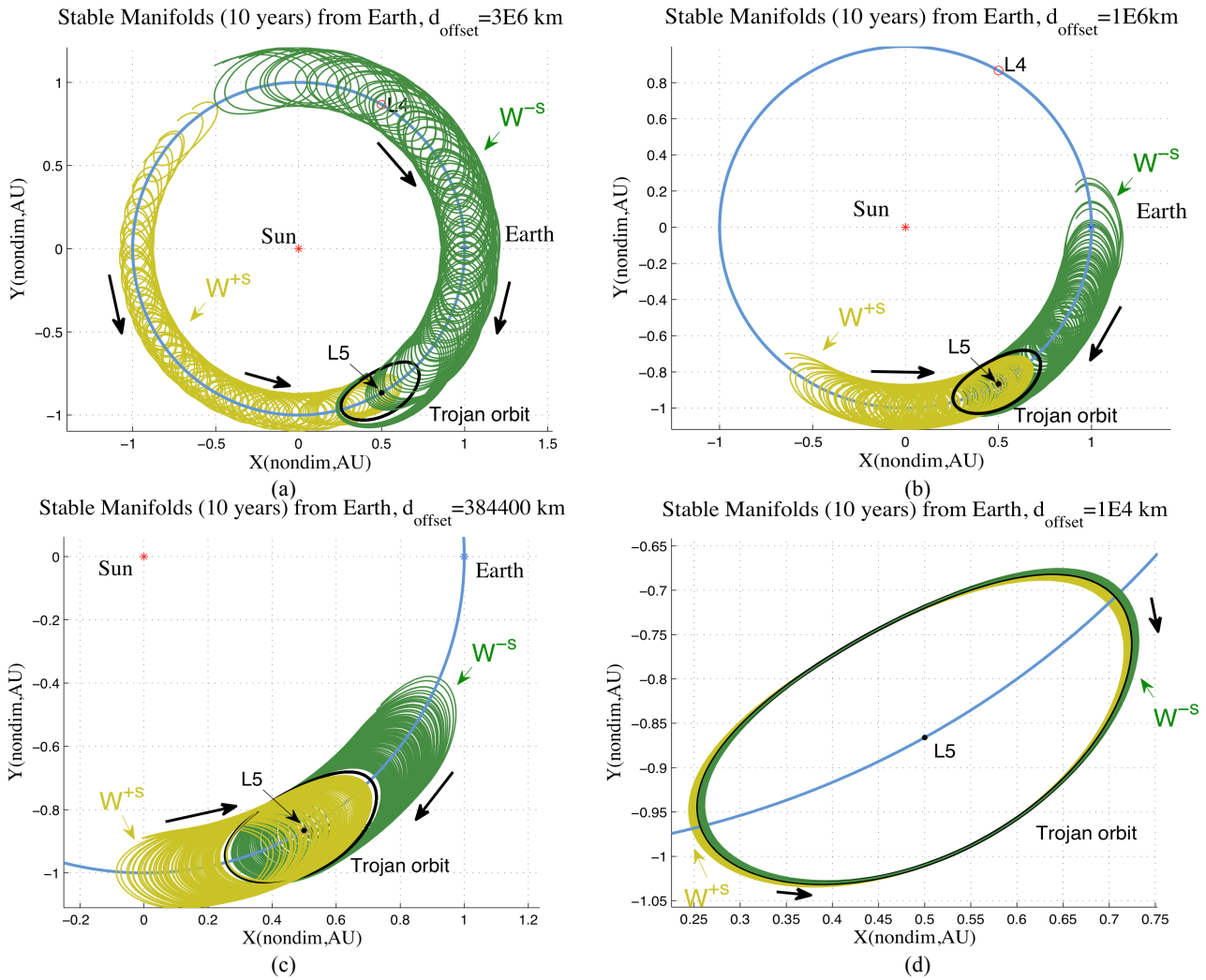

Fig. 3 Stable manifolds L5. These trajectories are integrated backwards in time from the Trojan orbit. Thus, the trajectory forward in time is the trajectory that the spacecraft would follow in reality. The problem is that these trajectories are too long and not suitable for transfers from Earth. (a) Manifolds generated with an offset of 3×10^6 km; (b) manifolds generated with an offset of 1×10^6 km (c) manifolds generated with an offset of 384,400 km (Earth-Moon distance); (d) manifolds generated with an offset of 1×10^4 km.

unsuitable for transfers from the Earth. Therefore, the results shown in this paper provide an insight on how to transfer from one triangular point to the other using powered flight (ΔV) as a way to speed up the transfer time.

5. L5-L4 and L4-L5 Heteroclinic Connections

Fig. 4 exhibits a long powered heteroclinic connection between L4-L5 and Fig. 5a shows a L5-L4 heteroclinic connection. The long L4-L5 transfer takes 1,685.6 days and requires an injection ΔV of 897.4 m/s to depart from the Trojan orbit (amplitude of 0.73 AU) around L4 and a ΔV of 867.8 m/s to insert into the Trojan orbit (0.73 AU amplitude) around L5. The tick marks in Figs. 4 and 5a are separated by 30 days and 60 days, respectively. In the heteroclinic connection shown in Fig. 5a, the departing ΔV from L5 is about 1.860 km/s while the insertion ΔV required into L4 is about 1.697 km/s.

Fig. 5b displays a short L4-L5 powered heteroclinic connection with a time of flight of 596.6 days. The spacecraft departs from the same Trojan orbit around L4 as in the previous case, but it requires a larger injection burn of 2,426.7 m/s and it arrives at a Trojan

orbit around L5, where it needs an insertion burn of 2,366.7 m/s. The tick marks depicted in Fig. 5b are separated by 30 days.

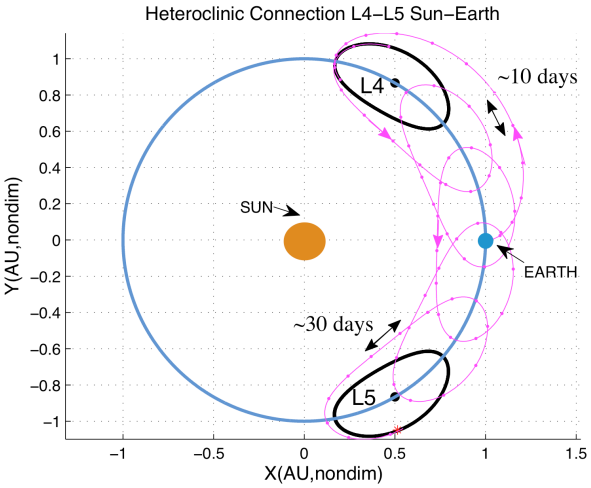

Fig. 4 Long powered heteroclinic connections between the triangular points L4 and L5 in the Sun-Earth system. Every loop or bounce is one Earth year-long. The time of flight of this heteroclinic connection is 1,685.59 days. The spacecraft requires 897.4 m/s to depart from a Trojan orbit (0.72 AU) around L4 and arrives at a Trojan orbit (0.72 AU) around L5, requiring 867.8 m/s at insertion.

This trajectory loops around the Earth, having the possibility of connecting to a quasi-satellite orbit at the intersection points of the heteroclinic transfer orbit and the quasi-satellite orbit (green oval orbit) from Fig. 2a.

In Figs. 6a and 6b, we show two short L4-L5 powered heteroclinic connections of 243.4 days and 460.9 days, respectively.

Although the transfer time of the trajectories as shown in Figs. 5 and 6 is very short, the total ΔV required for both heteroclinic transfers are about 12 km/s and 13 km/s, respectively.

6. L5-L3 Heteroclinic and Homoclinic Connections

In Fig. 7a, we show a homoclinic connection where the satellite departs from an asymmetric orbit with a 342 m/s injection burn and a time of flight of about 14 years. Then it stays for about 2 years before returning counterclockwise towards the same vicinity of the asymmetric orbit. The time of flight of the return trajectory is 8 years. Although not shown here, the spacecraft would need an insertion burn at the return to the asymmetric orbit.

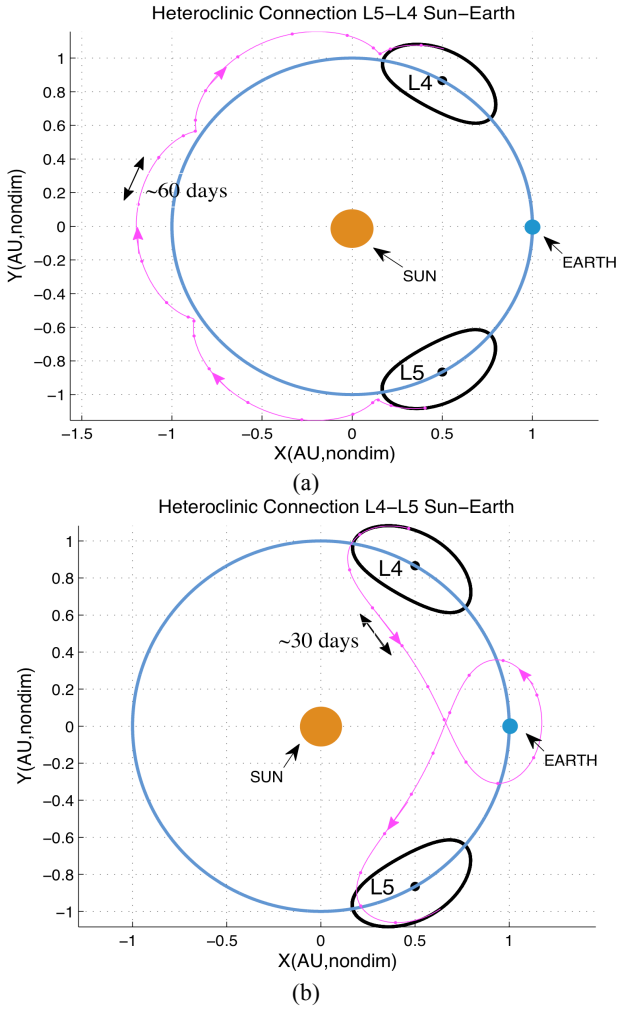

Fig. 5 (a) Powered heteroclinic connection from L5 to L4 of 1,583.14 days. The transfer orbit is clockwise and outside the path of the Earth around the Sun; (b) short heteroclinic connection between the triangular points L4 and L5 in the Sun-Earth system. The satellite loops around the Earth before heading towards the Trojan orbit around L5. The time of flight is 596.62 days. The spacecraft needs 2.426 km/s when departing L4 and 2.367 km/s at insertion into the Trojan orbit around L5.

For the heteroclinic connections displayed in Fig. 7b, the spacecraft can orbit the vicinity of L3 for about 28 years and it does not need any deterministic maneuvers to be captured around L3. However, the satellite requires an injection burn at the sub-L5 orbit of about 730 m/s for the red trajectory and 536 m/s for the purple trajectory. After this time, the spacecraft moves away from the vicinity of L3 clockwise

towards L4 for the trajectory in red and counterclockwise for the trajectory in purple as shown

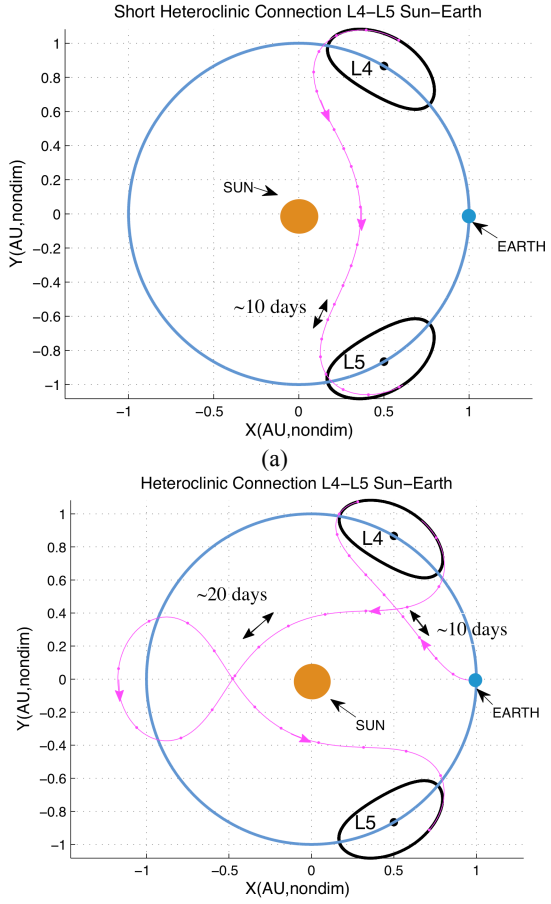

Fig. 6 Short powered heteroclinic connections between the triangular points L4 and L5 in the Sun-Earth system. Every loop or bounce is one Earth year-long. (a) Shortest heteroclinic connection with a time of flight of 243.42 days. The spacecraft requires 6.083 km/s to depart from a Trojan orbit (0.72 AU) around L4 and arrives at a Trojan orbit (0.72 AU) around L5, requiring 6.088 km/s at insertion; (b) heteroclinic connection from L4 to L5 of 460.93 days which requires 6.591 km/s and 6.424 km/s to depart L4 and insert into L5, respectively.

in Fig. 8 (amplified section of Fig. 7b and Fig. 7c).

Similarly, the powered heteroclinic connection displayed in Fig. 7c illustrates a satellite leaving L5 with a required burn of only 299 m/s, arriving 11 years later in the vicinity of L3 with a stay time of about 6 years. After this time, the satellite follows a counterclockwise motion around the Sun towards L4.

Other quasi-periodic orbits were also analyzed around L3 with amplitudes large enough (0.1 AU or larger as seen in Fig. 7) so that a spacecraft will be able to communicate directly [12] with Earth and without being occulted by the Sun. An amplified section of the orbits around L3 is illustrated in Fig. 8. Although these orbits do not require an insertion burn into the L3 orbits in the CRTBP, the spacecraft may need minor station-keeping maneuvers when using a high fidelity ephemeris model.

A spacecraft in one of these orbits will obtain observations of CMEs coming from behind the Sun (as seen from the Earth) that can not yet be seen by a spacecraft at L1 and therefore will have the advantage of earlier warnings when the CME or any other solar event travels along the Parker spiral (magnetic field sheet twisted when the Sun rotates) within the corotating zone.

7. Quasi-Satellite Orbits

Perhaps one of the most attractive orbits for solar observations is the quasi-satellite orbit depicted in Fig. 9a. The satellite departs from a 200 km parking orbit around the Earth with an injection burn of 3.613 km/s. The transfer time to the insertion into the quasi-satellite orbit (A_x = 0.425 canonical units or 63,833,411 km and A_y = 0.825 canonical units or 127,666,828 km) is about 245.8 days, requiring an insertion ΔV of 3.07 km/s. Among all the trajectories that were explored by varying slightly the velocity at injection up to 1%, we found that our lowest ΔV solution (not optimized) of 3.07 km/s corresponds to X = 1.132251 AU and Y = -0.008929 AU as we illustrate in Fig. 9b. A red star indicates the insertion burn into the QSO. Other trajectories were also obtained for shorter times of flight but at the expense of very high insertion ΔVs, which may not be suitable for mission design purposes for current propulsion systems. The trajectories of the probe intersect the quasi-satellite orbit at different points so each trajectory will also have a different time of flight. In Fig. 9c, we display ΔV-insertion into the QSO for a given transfer time. The QSO was integrated over the time span of 20 years. Fig. 9c displays the ΔV insertion, in km/s, of

possible transfer integrated trajectories shown in magenta in Fig. 9a.

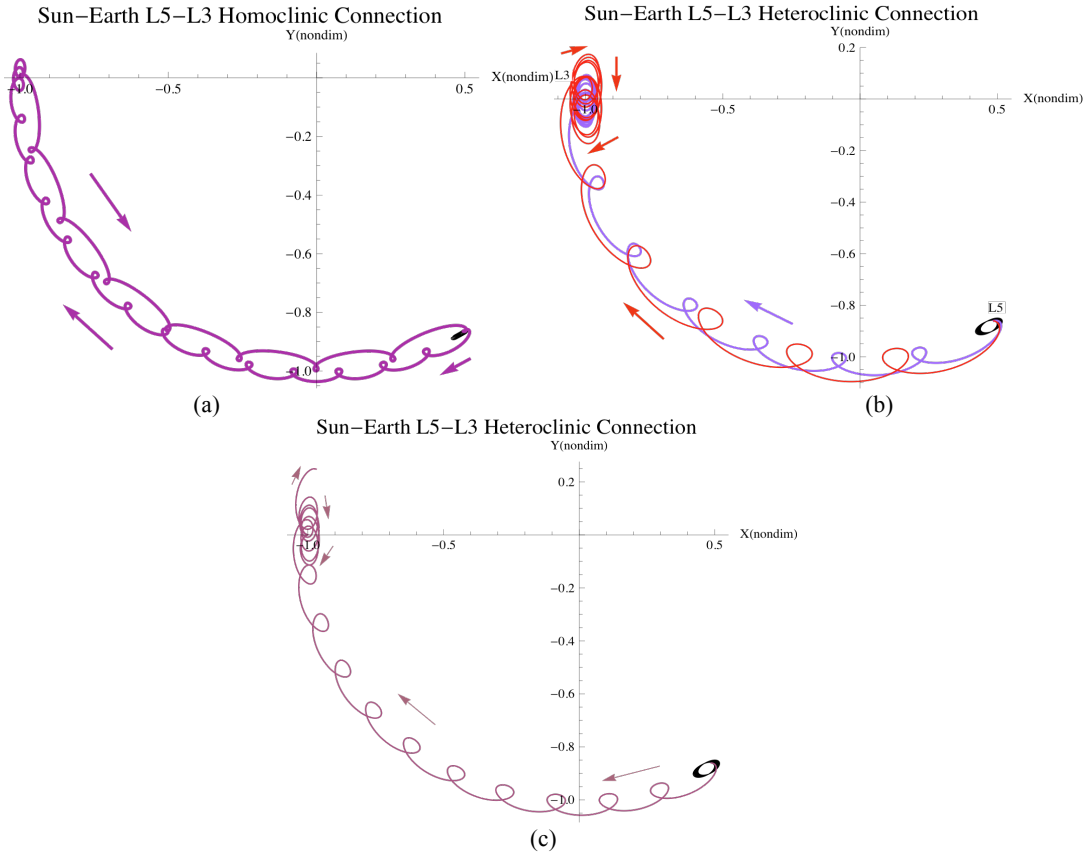

Fig. 7 (a) Long homoclinic connection between L5 and L3; (b) short heteroclinic connections between the triangular points L5 and L3 in the Sun-Earth system of 6 years (red) and 7 years (purple); (c) long heteroclinic connection from L5 to L3 of 11 years. A spacecraft placed around any of these orbits around the collinear point L3 will provide continuous monitoring of solar conditions.

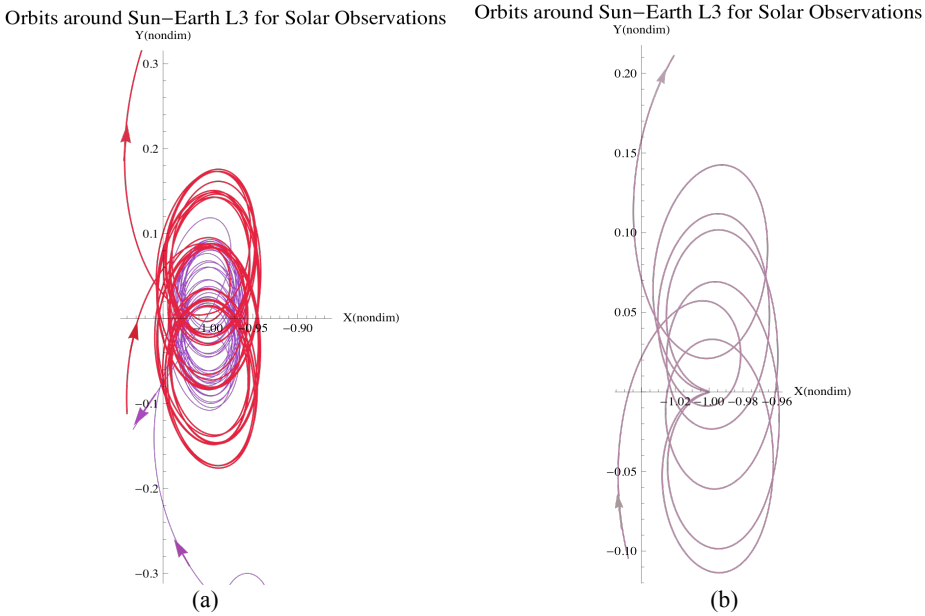

Fig. 8 Large amplitude orbits around L3 in the Sun-Earth system. (a) Maximum amplitude excursions of about 0.1-0.18 AU; (b) maximum amplitude excursions of about 0.15 AU.

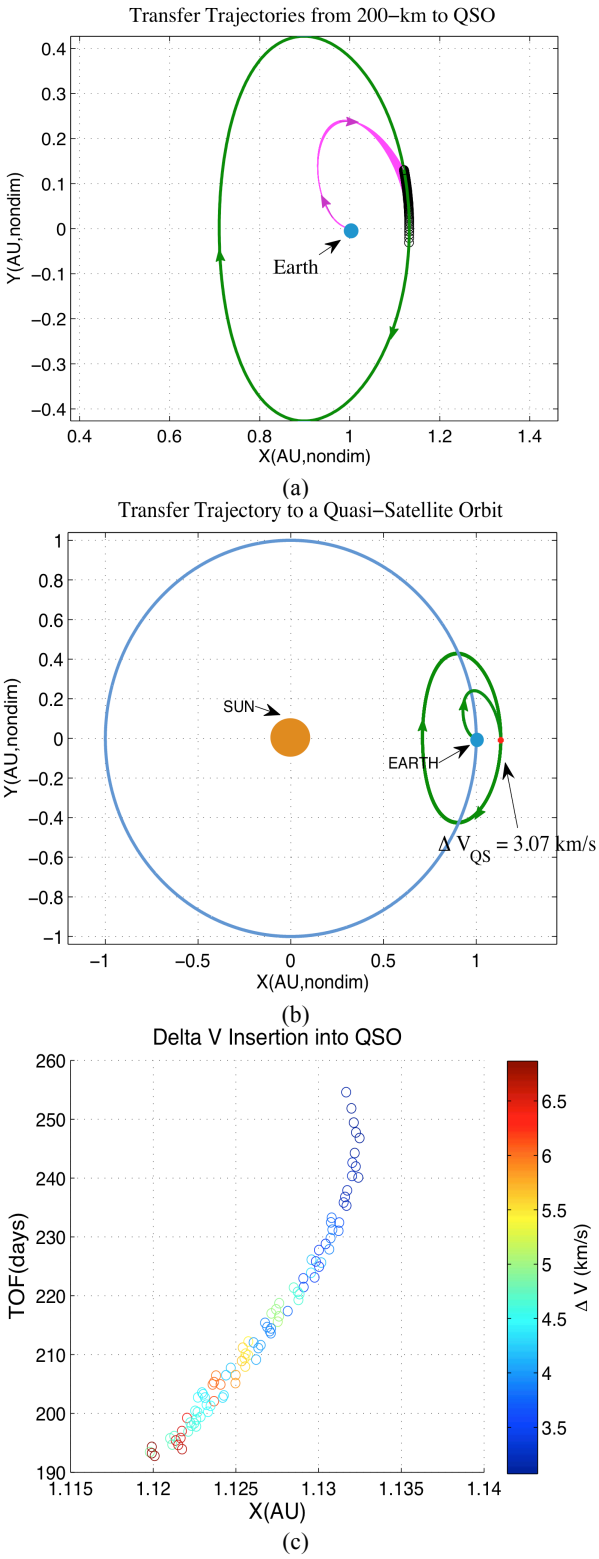

Fig. 9 (a) Transfer trajectories from Earth (200 km) to a QSO; (b) transfer trajectory with a time of flight of 245.8 days and an insertion burn, indicated by a red star, ΔV_{QS}, of 3.07 km/s; (c) ΔV insertion in km/s of transfer trajectories (magenta) shown in Fig. 9a.

The spacecraft is inserted into the quasi-satellite orbit that has been numerically integrated over 20 years, showing very good stability properties for very long periods of time. We also analyzed the invariant manifolds from the quasi-satellite orbit. Given the stability properties of this QSO, the orbits departing (unstable manifolds) from the QSO or arriving (stable manifolds) to the QSO have small orbit drifts of less than 200,000 km when the perturbation from the QSO is 1,000 km (standard perturbations are of the order of 200 km when computing the invariant manifolds around the collinear points in the Sun-Earth system). When considering very large perturbations of the order of an Earth-Moon distance, these trajectories obviously drift much more (Figs. 10a and 10b). The integration over 5 years included 50 trajectories for each manifold.

Another possibility for transferring to a quasi-satellite orbit is via the powered heteroclinic connection between the triangular points in the Sun-Earth system as observed in Fig. 11. There are four locations (indicated by red dots) where deterministic maneuvers can be performed to transfer the spacecraft from this heteroclinic connection into the QSO.

In this particular case, the heteroclinic transfer departs from the Trojan orbit around L4 towards L5 so the insertion into the QSO would be such that the spacecraft would have a direct motion. Another scenario (not shown) would be an heteroclinic connection departing from the Trojan orbit around L5 (and their corresponding transfer orbits [7, 10] from Earth) so that the spacecraft would follow a retrograde motion after insertion into the QSO.

The quasi-satellite orbit (green) analyzed in Fig. 12 is symmetric about the Sun-Earth direction. This quasi-satellite orbit (magenta) can also be found displaced (in the direction of L4) from the Sun-Earth direction as illustrated in Fig. 12. In this case, the spacecraft has a direct motion around the QSO. The transfer trajectory started from a 200 km orbit with an

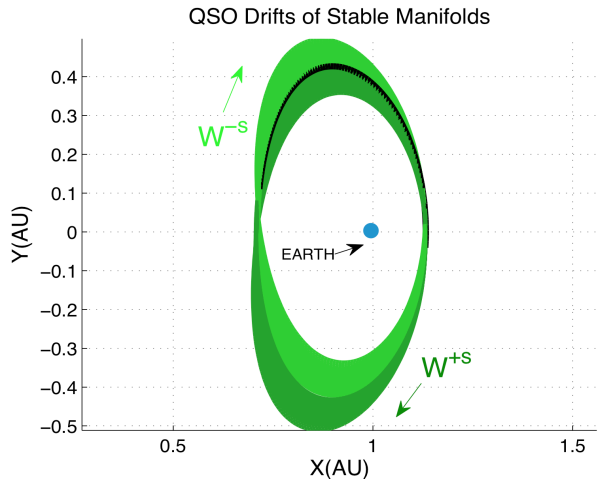

Fig. 10 (a) Stable invariant manifolds for large QSO perturbation; (b) unstable invariant manifolds. The black orbit represents the QSO (quasi-satellite orbit).

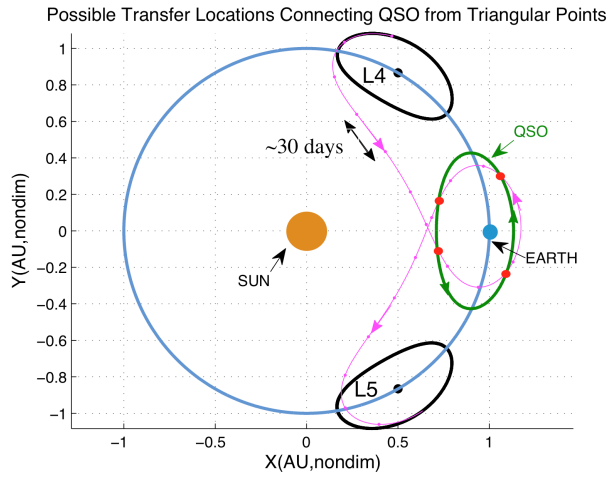

Fig. 11 Locations (red dots) where possible maneuvers can be performed to transfer the spacecraft between the triangular points heteroclinic connection into a QSO in the Sun-Earth system.

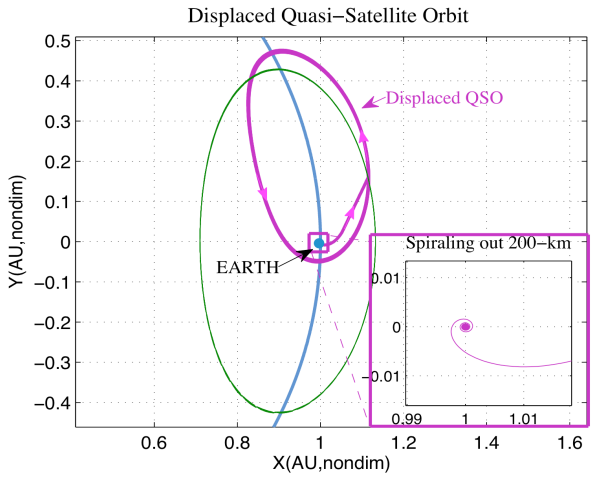

Fig. 12 Displaced QSO (purple) in the Sun-Earth system.

initial mass of 10,600 kg. The thrust is performed during a time period of about 65 days consuming a total of about 2,054 kg. This leaves a spacecraft wet mass of 8,546 kg on arrival to the QSO, which corresponds to a similar mass of the first Chinese space station, Tiangong 1, of about 8,500 kg. Similarly, orbits (not shown) displaced towards L5 can also be found with the spacecraft having a retrograde motion around the QSO.

There seem to be other attractive orbits not only for weather observations but also for searching for new undiscovered asteroids that can be captured in some of these displaced QSO, which may be either displaced upstream or downstream the Sun-Earth line.

8. Conclusions

Trojan orbits and sub-L5 orbits were previously found as potential locations for space weather monitoring since they can anticipate weather up to one week in advance before solar events actually arrive at Earth. In this paper, we have investigated new orbit geometries, such as powered heteroclinic and homoclinic connections between the triangular points and the collinear points in the Sun-Earth system.

Some of these trajectories are powered heteroclinic connections linking L4 and L5 for a total ΔV (departure and arrival) of less than 1.8 km/s. This type of trajectory loops around the Earth so material could be transported not only between the triangular points

but also between these trajectories and the QSO (quasi-satellite orbits) described in this work. Other heteroclinic connections are also possible between the L_5 and the collinear point L3 in the Sun-Earth system. The total ΔV required for some of these trajectories can be as low as 299 m/s and as high as 730 m/s, depending on the time of transfer and the size of the initial orbit around L5. These orbits are very attractive from the science perspective because a probe could monitor space weather without interruptions once it orbits the vicinity of L3 with amplitudes of about 0.01 AU (1,500,000 km) to 0.18 AU (27,000,000 km) and therefore, could be used during the end of life of the spacecraft. The spacecraft would not need any deterministic maneuvers to be captured into the L3 vicinity because it will be captured without a maneuver. The probe will stay in the vicinity of L3 for many years before being ejected out of this neighborhood either towards the L4 point (similar to the motion of asteroid 2010 TK7) or back to the L5 vicinity again. These are examples of heteroclinic and homoclinic connections that can be used in future space missions for reconnaissance purposes where the spacecraft will tour different libration points.

In this paper, we also investigated other orbit geometries (QSO) as promising orbits where to place a spacecraft for solar observations purposes. These orbits are in 1:1 resonance with the motion of Earth around the Sun from where several small spacecraft will be able to provide continuous solar observations from a sub-L1 perspective and be able to anticipate space weather many hours or even one to two days in advance of reception at a L1 position. Quasi-satellite orbits can also be displaced either upstream or downstream from the Sun-Earth line and therefore could be tailored accordingly to the mission requirements.

We are constantly intrigued by the different families of orbits that we can find and we may be able to find in the future. Besides the Trojans orbits around L5, sub-L5 orbits, tadpole orbits, horseshoe orbits described in past work, this work describes very attractive powered heteroclinic and homoclinic connections between the triangular points and collinear points in the CRTBP of the Sun-Earth system and quasi-satellite orbits for solar observations.

Acknowledgments

The research was partially performed at the Astronautical Engineering Department, the Viterbi School of Engineering of the University of Southern California. Part of this work described in this paper was carried out during the Jet Propulsion Laboratory SURP (Strategic University Research Partnership) 2010 Program, California Institute of Technology under a contract with the National Aeronautics and Space Administration. This work has been partially supported by the Marie Curie fellowship PITN-GA-2011-289240 Astronet-II.

References

[1] J.S. Parker, M. W. Lo, Shoot the moon 3D, Advances in the Astronautical Sciences 123 (2006) 2067-2086.

[2] G. Gómez, W.S. Koon, M.W. Lo, J.E. Marsden, J. Masdemont, S.D. Ross, Connecting orbits and invariant manifolds in the spatial restricted three-body problem, Nonlinearity 17 (2004) 1571-1606.

[3] J.K. Miller, Lunar Transfer Trajectory Design and the Four Body Problem, in: AAS/AIAA Astrodynamicist Specialist Conference, Ponce, Feb. 9-13, 2003, pp. 3-144.

[4] M. Connors, P. Wiegert, C. Veillet, Earth's First Trojan Asteroid: 2010 TK7, Athabasca University, the University of Western Ontario and the Canada-France-Hawaii Telescope, http://www.astro.uwo.ca/~wiegert/2010TK7 (accessed June 12, 2013).

[5] P.J. Llanos, J.K. Miller, G.R. Hintz, Mission and navigation design of integrated trajectories to L4,5 in the Sun-Earth system, in: AIAA/AAS Astrodynamicist Specialist Conference, Minneapolis, AIAA 2012-4668, Aug. 13-16, 2012.

[6] P.J. Llanos, J.K. Miller, G.R. Hintz, Navigation analysis for an L5 mission in the Sun-Earth system, in: AAS/AIAA Astrodynamicist Specialist Conference, Girdwood, Vol. 142, July 31-Aug. 4, 2011, pp. 11-503.

[7] P.J. Llanos, J.K. Miller, G.R. Hintz, L5 Mission design

targeting strategy, in: AAS/AIAA Astrodynamicist Specialist Conference, Kauai, Feb. 10-14, 2013, pp. 13-223.

[8] K.C. Howell, Three-dimensional periodic halo orbits, Celestial Mechanics 32 (1984) 53-71.

[9] The MITRE corporation JASON, impacts of severe space weather on the electric grid, JSR-11-320 Report [Online], November, 2011, http://www.fas.org/irp/agency/dod/jason/spaceweather.pdf (accessed June 12, 2013).

[10] M.W. Lo, P.J. Llanos, G.R. Hintz, An L5 mission to observe the sun and space weather, in: AAS/AIAA Astrodynamicist Specialist Conference, San Diego, Part I, Vol. 136, Feb. 14-18, 2010, pp. 10-121.

[11] A.E. Petropoulos, J.M. Longuski, Shape-based algorithm for automated design of low-thrust, gravity-assist trajectories, Journal of Spacecraft and Rockets 41 (5) (2004) 787-796.

[12] M. Tantardini, E. Fantino, R. Yuan, P. Piergola, G. Gómez, J.J. Masdemont, Spacecraft trajectories to the L3 point of the Sun-Earth Three-Body problem, Celestial Mechanics Dynamical Astronomy 108 (2010) 215-232.